Targeting ectromelia virus and TNF/NF-κB or STAT3 signaling for effective treatment of viral pneumonia

Pratikshya Pandey[a,1], Zahrah Al Rumaih[b,1], Ma. Junaliah Tuazon Kels[b,1], Esther Ng[b], Rajendra Kc[a], Geeta Chaudhri[b,2], and Gunasegaran Karupiah[a,b,2,3]

[a]Viral Immunology and Immunopathology Group, Tasmanian School of Medicine, University of Tasmania, Hobart, TAS 7000, Australia; and [b]Department of Immunology, John Curtin School of Medical Research, Australian National University, Canberra, ACT 2601, Australia

Edited by Bernard Moss, Laboratory of Viral Diseases, National Institute of Allergy and Infectious Diseases, Bethesda, MD; received July 12, 2021; accepted January 13, 2022

Viral causes of pneumonia pose constant threats to global public health, but there are no specific treatments currently available for the condition. Antivirals are ineffective when administered late after the onset of symptoms. Pneumonia is caused by an exaggerated inflammatory cytokine response to infection, but tissue necrosis and damage caused by virus also contribute to lung pathology. We hypothesized that viral pneumonia can be treated effectively if both virus and inflammation are simultaneously targeted. Combined treatment with the antiviral drug cidofovir and etanercept, which targets tumor necrosis factor (TNF), downregulated nuclear factor kappa B–signaling and effectively reduced morbidity and mortality during respiratory ectromelia virus (ECTV) infection in mice even when treatment was initiated after onset of clinical signs. Treatment with cidofovir alone reduced viral load, but animals died from severe lung pathology. Treatment with etanercept had no effect on viral load but diminished levels of inflammatory cytokines and chemokines including TNF, IL-6, IL-1β, IL-12p40, TGF-β, and CCL5 and dampened activation of the STAT3 cytokine-signaling pathway, which transduces signals from multiple cytokines implicated in lung pathology. Consequently, combined treatment with a STAT3 inhibitor and cidofovir was effective in improving clinical disease and lung pathology in ECTV-infected mice. Thus, the simultaneous targeting of virus and a specific inflammatory cytokine or cytokine-signaling pathway is effective in the treatment of pneumonia. This approach might be applicable to pneumonia caused by emerging and re-emerging viruses, like seasonal and pandemic influenza A virus strains and severe acute respiratory syndrome coronavirus 2.

viral pneumonia | respiratory ectromelia virus infection | dysregulated inflammatory cytokine response | combined antiviral and anti-inflammatory drug treatment | TNF/NF-κB and STAT3 signaling pathways

Pneumonia is a serious complication caused by inflammation of the lungs due to infection with diverse viral pathogens that often results in respiratory failure and death (1, 2). It is caused by an exaggerated inflammatory response associated with dysregulated inflammatory cytokine production, also known as cytokine storm, and leukocyte infiltration (3, 4). There are no specific treatments available for pneumonia caused by viruses.

Antivirals are not effective in protecting against severe disease, particularly when treatment is administered late (>48 h) after the onset of symptoms. Most individuals may not seek medical attention within this timeframe. At that stage of the disease, tissue damage due to high viral load and excessive inflammation contributes to lung pathology, morbidity, and mortality. We reasoned that the simultaneous targeting of both virus and inflammation might be an approach to effectively treat viral pneumonia (3).

We used the mousepox model to establish proof of concept that targeting both virus and inflammation late after disease onset might be more effective in reducing morbidity and mortality. Ectromelia virus (ECTV), the agent of mousepox, is a small animal model for smallpox caused by variola virus (VARV) in humans. ECTV and VARV are related orthopoxviruses (OPXV) that can be transmitted through the respiratory route and cause severe pneumonia associated with cytokine storm, inflammation, lung pathology, and death (5, 6). We focused on tumor necrosis factor (TNF) for three reasons. First, it is one of the earliest inflammatory cytokines to be produced following viral infection through activation of the nuclear factor kappa B (NF-κB)–signaling pathway (7, 8). Second, TNF plays a critical role in driving lung inflammation, severe pathology, and death during respiratory viral infections caused by VARV, influenza A virus (IAV), severe acute respiratory syndrome coronavirus 2 (SARS-CoV-2), and respiratory syncytial virus (RSV) (9–12). Third, ECTV-encoded TNF receptor (TNFR) homolog, termed cytokine response modifier D, mediates potent anti-inflammatory activity in vivo (10, 13). Hence, we predicted that exogenous anti-TNF reagents should also be effective in dampening lung inflammation during respiratory ECTV infection.

TNF is produced as a membrane-bound protein (mTNF) from which the soluble form (sTNF) is released via proteolytic cleavage by metalloprotease enzymes (14). Both sTNF and

Significance

Antivirals are ineffective in treating viral pneumonia if administered after 48 h post onset of disease symptoms. Lung pathology during respiratory viral infections is triggered by the host inflammatory response and tissue damage caused by replicating virus. Therefore, targeting both virus and inflammation would be more effective in treating pneumonia. Simultaneous treatment with an anti-inflammatory drug targeting TNF or STAT3 combined with an antiviral drug significantly improved clinical disease, reduced lung viral load and pathology and protected mice from severe pneumonia caused by respiratory ectromelia virus infection. The combined treatment suppressed multiple proinflammatory cytokines and cytokine-signaling pathways, including NF-κB and STAT3. Late after onset of symptoms, antiviral treatment alone cannot ameliorate viral pneumonia, as it cannot reduce inflammation effectively.

Author contributions: P.P., Z.A.R., M.J.T.K., E.N., G.C., and G.K. designed research; P.P., Z.A.R., M.J.T.K., E.N., and R.K. performed research; P.P., Z.A.R., M.J.T.K., E.N., G.C., and G.K. analyzed data; P.P., G.C., and G.K. wrote the paper; M.J.T.K. and R.K. commented on first draft; and G.C. and G.K. provided funding acquisition.

The authors declare no competing interest.

This article is a PNAS Direct Submission.

This article is distributed under Creative Commons Attribution-NonCommercial-NoDerivatives License 4.0 (CC BY-NC-ND).

[1]P.P., Z.A.R., and M.J.T.K. contributed equally to this work.

[2]G.C. and G.K. contributed equally to this work.

[3]To whom correspondence may be addressed. Email: Guna.Karupiah@utas.edu.au.

This article contains supporting information online at http://www.pnas.org/lookup/suppl/doi:10.1073/pnas.2112725119/-/DCSupplemental.

Published February 17, 2022.

mTNF function by binding to either of two receptors, TNFRI or TNFRII. The binding of sTNF to TNFRI or TNFRII delivers a forward signal. However, when bound to TNFR, mTNF can also function as a receptor and transmit signals into mTNF-bearing cells, a process termed reverse signaling (3). During respiratory ECTV infection, mTNF alone is necessary and sufficient to regulate lung inflammation and pathology (6). Excessive or an absence of TNF results in the dysregulation of an overlapping set of cytokine-signaling pathways, including the NF-κB and signal transducer and activator of transcription (STAT) 3 pathways (6, 13). We thus posited that blockading a specific inflammatory cytokine like TNF or a cytokine-signaling pathway like STAT3 (downstream of TNF/NF-κB signaling) would result in similar outcomes. The NF-κB- and STAT3-signaling pathways cross-regulate each other and regulate an overlapping set of inflammatory genes (15, 16), and therefore, targeting either pathway might result in a reduction in lung inflammation.

We have found that the antiviral drug cidofovir, a nucleoside analog that inhibits viral DNA replication, effectively reduces morbidity and mortality in ECTV-infected mice even at an extended time period after onset of clinical disease but only if inflammation is also targeted simultaneously. We used the anti-TNF drug, etanercept, which is widely used to treat several inflammatory diseases (17, 18). The combined therapy reduced lung viral load, inflammation, and pathology and significantly increased survival rates of mice from an otherwise lethal infection. Treatment with the antiviral alone was effective in reducing viral load but animals died nonetheless from severe lung inflammation and pathology. Additionally, treatment with the anti-inflammatory drug reduced lung pathology but did not protect the animals. Multiple doses of the inflammatory drug were necessary for the combined treatment to be effective.

We made a similar finding when an inhibitor of STAT3 (S3I-201) was used instead of etanercept to reduce lung inflammation in cidofovir-treated mice. The combined treatment was effective even in TNF-deficient ($TNF^{-/-}$) mice, in which etanercept had no effect, indicating that STAT3 inhibition will be more appropriate for individuals who cannot be treated with etanercept due to contraindications or when TNF is not the driver of lung inflammation. This approach to treating pneumonia might be applicable to pneumonia caused by other respiratory viral infections, including IAV, RSV, and SARS-CoV-2.

Results

Combined Treatment with Etanercept and Cidofovir Reduces Weight Loss, Clinical Signs, Lung Pathology, and Leukocyte Infiltration. Intranasal (i.n.) instillation of ECTV in mice produces signs of respiratory disease between 4 and 8 d postinfection (p.i.) depending on virus dose and manifests as pneumonia with severe lung pathology around 6 to 10 d (6, 13). In this experiment, ECTV was used at a dose that was sublethal for wild-type (WT) mice, but a comparable dose is lethal in $TNF^{-/-}$ mice due to dysregulated cytokine responses and exacerbated lung pathology, but it is not due to increased viral load (6, 13).

We used WT and $TNF^{-/-}$ C57BL/6 mice to first establish that the anti-TNF drug, etanercept, was effective in the ECTV model. $TNF^{-/-}$ mice were used as controls, since etanercept would not be effective in this strain. Mice were infected and treated with etanercept on days 1, 4, and 7 p.i. Clinical scores were generated based on the condition of hair coat, posture, breathing, lacrimation and nasal discharge, and activity and behavior as described elsewhere (6, 13). Microscopic examination of hematoxylin and eosin (H&E)–stained lung histological sections were used to generate histopathological scores as described previously (6, 13).

Etanercept treatment had minimal effects on weight loss (*SI Appendix*, Fig. S1 *A* and *B*) but significantly reduced clinical disease in WT but not in $TNF^{-/-}$ mice (*SI Appendix*, Fig. S1 *C* and *D*). It had no effect on survival rates in both strains over the 9-d study period (*SI Appendix*, Fig. S1 *E* and *F*). Etanercept reduced histopathological scores in WT but not in $TNF^{-/-}$ mice (*SI Appendix*, Fig. S1*G*), which expectedly succumbed to mousepox beginning at day 8 p.i., but it had no effect on viral load (*SI Appendix*, Fig. S1*H*).

We tested our hypothesis that reducing inflammation after the onset of disease signs will make the antiviral treatment more effective in reducing morbidity. The timing of initiation of combined treatment and termination of experiments in this study depended on the virus strain and dose used (Naval versus Moscow; sublethal versus lethal), how rapidly the animals fell sick, and the animal ethics requirements at the institutions where experiments were performed, and these are detailed in *Materials and Methods* and summarized in Fig. 1. We used sublethal and lethal doses of virus to determine whether the relationship between pathology caused by the inflammatory response and virus-induced pathology are comparable during sublethal and lethal infection.

Mice infected with a sublethal dose of ECTV were treated with etanercept, cidofovir, or both drugs (combined treatment) on day 6 p.i. (24 h after the onset of disease signs). Etanercept was administered again on day 8 to the relevant groups, and all animals were euthanized on day 10.

Cidofovir or cidofovir plus etanercept (combined) treatment significantly reduced weight loss in $TNF^{-/-}$ mice but had no effect in WT mice (Fig. 2 *A* and *B*). Etanercept alone was not effective in reducing weight loss in both strains of mice (Fig. 2 *A* and *B*). Treatment with cidofovir but not etanercept reduced clinical scores in both strains of mice (Fig. 2 *C* and *D*). However, the combined treatment was most effective in reducing clinical scores in WT mice, whereas cidofovir and combined treatment were equally effective in $TNF^{-/-}$ mice. Since ECTV causes systemic infection when inoculated through the i.n.

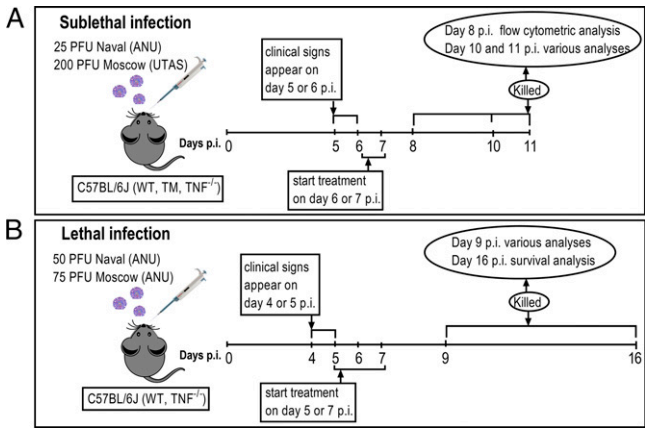

Fig. 1. Schematic diagram showing mouse strains, strains and doses of ECTV, timing of treatment initiation and termination, and analyses used in this study. C57BL/6 WT, $TNF^{-/-}$, or TM mice were anesthetized and infected intranasally with ECTV Moscow or Naval strains. (*A*) In experiments performed at the ANU, 25 PFU of ECTV (Naval) was a sublethal dose, whereas 200 PFU of ECTV (Moscow) was used as a sublethal dose at UTAS, with disease signs evident at days 5 to 6 p.i. (*B*) At the ANU, doses of 50 PFU Naval and 75 PFU Moscow strains of ECTV were found to be lethal and clinical signs were evident as early as day 4 p.i. The timing of treatment initiation and termination of experiments was depended on the virus strain and dose used and the animal ethics requirements at the institutions where the experiments were performed. Animals were weighed and clinically scored every day. Mice that were severely moribund with a clinical score of ≥10 and/or a body weight loss of ≥20% (UTAS) or 25% (ANU) were euthanized, tissues collected for analysis, and mice considered dead the following day.

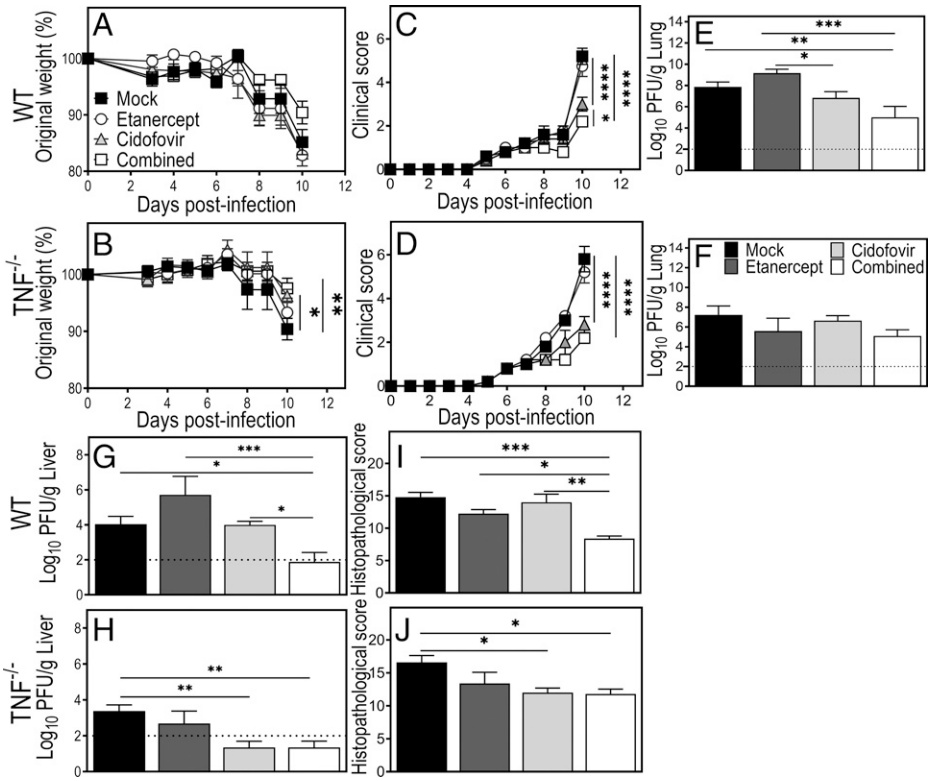

Fig. 2. Combined treatment with etanercept and cidofovir reduces clinical scores, viral load, and lung pathology in ECTV-infected WT mice. Age-matched groups of female WT and TNF$^{-/-}$ mice (n = 4 or 5) were infected with 25 PFU of ECTV Naval strain i.n. Animals were treated with etanercept, cidofovir, or both drugs (combined) on day 6 p.i., the relevant groups were treated one more time with etanercept on day 8, and animals were euthanized on day 10 p.i. Weight loss (*A* and *B*) and clinical scores (*C* and *D*) were monitored during the course of infection, analyzed using two-way ANOVA with Sidak's posttest. Lung and liver viral load data (*E–H*) were log transformed and analyzed using one-way ANOVA test followed by Fisher's least significant difference (LSD) test. Histopathological scores (*I* and *J*) are based on microscopic examination of lung histology H&E sections (presented in Fig. 3) and analyzed using one-way ANOVA test with Tukey's post hoc test. Data are expressed as means ± SEM *P < 0.05; **P < 0.01; ***P < 0.001, and ****P < 0.0001. Broken line in panels *E*, *F*, *G*, and *H* correspond to the limit of virus detection.

route, we measured viral load in lungs (Fig. 2 *E* and *F*) and livers (Fig. 2 *G* and *H*). As expected, viral load was significantly lower in livers than lungs, and etanercept treatment had no effect on viral titers in both strains of mice (Fig. 2 *E–H*). Cidofovir reduced lung viral load in WT mice, but the effect was even greater with combined treatment (Fig. 1*E*). Cidofovir had no apparent effect on lung viral load in TNF$^{-/-}$ mice, but liver titers were significantly reduced (Fig. 2*F*).

The histopathological scores were generated through assessment of lung H&E-stained histology sections shown in Fig. 3. The histopathological scores changed minimally in WT mice treated with either cidofovir or etanercept alone, but the combined treatment caused a significant reduction (Fig. 2*I*). In TNF$^{-/-}$ mice, cidofovir or the combined treatment reduced the histopathological scores, but etanercept alone had no effect (Fig. 2*J*).

Histologically, ECTV infection caused severe lung pathology with edema and destruction of bronchioles and alveoli in both strains of mice (Fig. 3 *A*, *B*, *I*, and *J*). As previously reported (6), lung pathology was worse in TNF$^{-/-}$ mice with complete alveolar wall collapse. Etanercept treatment reduced edema in WT but not in TNF$^{-/-}$ mice (Fig. 3 *C*, *D*, *K*, and *L*). Cidofovir reduced both parenchymal edema and alveolar/bronchiolar wall destruction in WT mice but only marginally in TNF$^{-/-}$ mice (Fig. 3 *E*, *F*, *M*, and *N*). The most-significant changes were seen in WT mice given the combined treatment (Fig. 3 *G* and *H*), which resulted in minimal edema and preservation of the alveolar walls. In TNF$^{-/-}$ mice, the combined treatment was not any more efficacious than treatment with only cidofovir (Fig. 3 *O* and *P*). The combined treatment with cidofovir and etanercept after the onset of disease signs was effective in significantly reducing clinical scores, viral load, and lung pathology in WT mice infected with a sublethal dose of virus.

We evaluated the effect of combination therapy on leukocyte recruitment to the lung. Mice infected with 25 plaque-forming units (PFU) ECTV i.n. were either mock treated or treated with cidofovir and etanercept (combined) on day 6 p.i. Animals were euthanized on day 8 p.i., and lung tissues were collected for flow cytometric analysis of leukocyte subsets following enzymatic digestion.

In WT mice, combined treatment with etanercept and cidofovir reduced numbers of leukocytes (CD45.2^{+}) infiltrating the lung (Fig. 3*Q*). There were reductions in F4/80^{+}, CD11b^{+}, and CD11b^{Hi}Ly6c^{Hi} leukocyte subsets (Fig. 3 *R–T*), but the other subsets were not affected (Fig. 3 *U–Z*). As inflammatory monocytes are CD11b^{Hi}Ly6c^{Hi} and can express F4/80, the reduction in leukocyte numbers might likely be a reflection of reduction in numbers of this leukocyte subset. In TNF$^{-/-}$ mice, with the exception of an increase in B cell (CD45R^{+}) numbers (Fig. 3*X*), combined treatment did not affect leukocyte recruitment to the lungs. As reported previously (6), there were no discernible differences in leukocyte numbers in mock-treated WT mice compared with TNF$^{-/-}$ mice.

Combined Treatment with Cidofovir and Single-Dose Etanercept Reduces Viral Load and Disease Severity but Not Lung Pathology during Sublethal Infection. Etanercept is administered once or twice a week to treat chronic inflammatory diseases such as

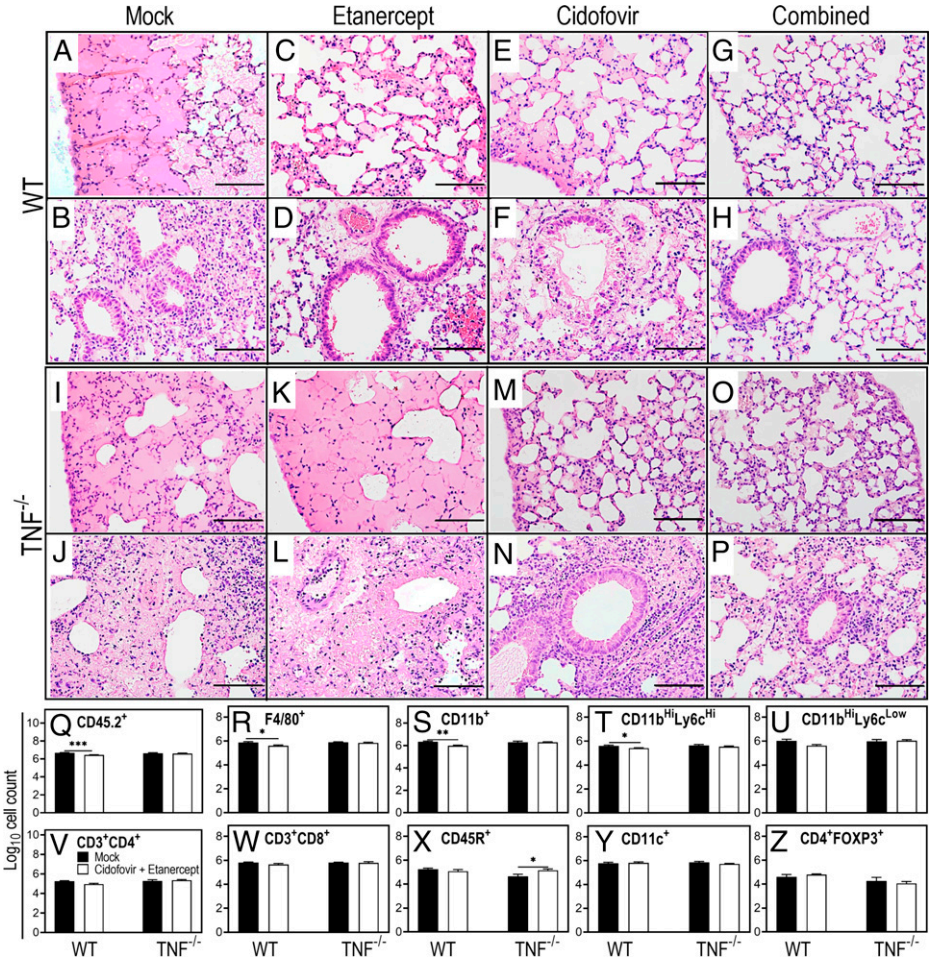

Fig. 3. Combined treatment with etanercept and cidofovir significantly reduces lung pathology and infiltration of inflammatory monocytes in WT mice but not TNF$^{-/-}$ mice. Lung tissue sections for histological examination were obtained from mice that were infected and treated as described in Fig. 1. Briefly, age-matched groups of female WT and TNF$^{-/-}$ mice were infected with 25 PFU ECTV (Naval) i.n. Etanercept, cidofovir, or both drugs (combined) were administered on day 6 p.i., and etanercept alone was administered again on day 8 to the relevant groups and animals were euthanized on day 10 p.i. Lungs were fixed in 10% neutral-buffered formalin, embedded in paraffin blocks, sectioned, and stained with H&E. Lung H&E sections of mock (*A*, *B*, *I*, and *J*), etanercept (*C*, *D*, *K*, and *L*), cidofovir (*E*, *F*, *M*, and *N*), and combined treatment (*G*, *H*, *O*, and *P*) groups were examined using bright-field microscope on all fields at 400× magnification. (Scale bars, 100 μm.) To assess the effect of combination therapy on immune cell recruitment to lungs, groups of four to five WT and TNF$^{-/-}$ mice were infected with 25 PFU of ECTV (Naval) i.n. At day 6 p.i., animals were treated with cidofovir plus etanercept and euthanized on day 8 p.i. The number of total leukocytes (*Q*) (CD45$^+$), macrophages (*R*) (F4/80$^+$), myeloid cells (*S*) (CD11b$^+$), inflammatory monocytes (*T*) (CD11b^{Hi}Ly6c^{Hi}), neutrophils (*U*) (CD11b^{Hi}Ly6c^{Low}), CD4$^+$ T cells (*V*) (CD3$^+$CD4$^+$), CD8$^+$ T cells (*W*) (CD3$^+$CD8$^+$), B cells (*X*) (CD45R$^+$), dendritic cells (*Y*) (CD11c$^+$), and regulatory T cells (*Z*) (CD3$^+$CD4$^+$CD25^{Hi}FOXP3$^+$) was determined in the digested lung tissue using flow cytometry. Data were log transformed, expressed as mean ± SEM, and analyzed using independent *t* test. **P* < 0.05 and ***P* < 0.01, relative to mock-treated group.

rheumatoid arthritis (19). Although the levels of TNF produced during an acute respiratory viral infection may be different to those during a chronic inflammatory disease, we investigated whether a single dose of etanercept might be sufficient to reduce lung pathology and morbidity in WT mice. As the dysregulated production of a number of inflammatory cytokines and chemokines correlated with severe lung pathology during respiratory ECTV infection (6, 13), we also investigated how the various treatment regimens modulated levels of inflammatory mediator(s) and whether those changes affected the correlation with disease severity. ECTV-infected mice were treated once at day 7 p.i. with cidofovir, etanercept, or both drugs and observed until day 11 p.i.

The combined therapy dramatically improved weight loss (*SI Appendix*, Fig. S2*A*) and clinical signs (*SI Appendix*, Fig. S2*B*), whereas the monotherapies had minimal impact on both parameters. Etanercept or cidofovir treatment had no effect on the lung viral load, but the combined treatment caused a significant reduction in ECTV titers (*SI Appendix*, Fig. S2*C*).

The lung histopathological scores were similar in mock- and etanercept-treated groups (*SI Appendix*, Fig. S2*D*). Cidofovir or the combined treatment reduced histopathological scores, but the changes were not significant compared to the mock treatment group. Thus, although a single dose of etanercept in the combined-treatment regimen significantly reduced weight loss, clinical scores, and viral load, it was not sufficient to cause a significant reduction in lung pathology.

One Dose of Etanercept Is Ineffective in Dampening Inflammatory Cytokines and pSTAT3 in the Lung. It was important to determine why a single dose of etanercept was not effective in reducing lung pathology. The binding of etanercept to sTNF will neutralize the cytokine, whereas when bound to mTNF expressed on cells, it can participate in reverse signaling, a process whereby the production of a number of inflammatory cytokines and NF-κB activation are inhibited or reduced (13, 20–22). We used lung tissue from the experiment described in *SI Appendix*, Fig. S2 to measure gene and protein expression levels for a number

of cytokines, chemokines, and phosphorylated (p) components of cytokine-signaling pathways, all of which have been implicated in contributing to lung pathology.

A single dose of etanercept reduced levels of messenger RNA (mRNA) transcripts for TNF but not any of the other inflammatory cytokines or chemokines (*SI Appendix*, Fig. S2 *E–L*). Cidofovir was more effective in that it reduced levels of TNF, interleukin (IL)-6, IL-1β, transforming growth factor (TGF)-β, and chemokine (C-C motif) ligand (CCL)5 (*SI Appendix*, Fig. S2 *E–G*, *I*, and *K*). Compared to cidofovir, the combined treatment was far more effective in reducing TNF and TGF-β (*SI Appendix*, Fig. S2 *E* and *I*), just as effective in reducing IL-1β and CCL5 (*SI Appendix*, Fig. S2 *G* and *K*), but less effective in reducing IL-6 levels (*SI Appendix*, Fig. S2*F*). None of the treatment regimens affected the levels of expression of IL-12p40, CCL2, or chemokine (C-X-C motif) ligand (CXCL)10 (*SI Appendix*, Fig. S2 *H*, *J*, and *L*).

TNF activates the NF-κB-signaling pathway, resulting in phosphorylation of the NF-κB p65 component (pNF-κB p65). Dysregulated activation of NF-κB can result in hyperactivation of STAT3, which can also cause lung pathology, and its inhibition substantially reduces the lung inflammatory response in ECTV-infected mice (6). We measured mTNF, sTNF, pNF-κB p65, and pSTAT3 proteins by Western blot analysis to determine how the various treatment regimens affected their levels of expression. Etanercept, cidofovir, and the combined treatment were all effective in reducing the levels of both mTNF and sTNF (*SI Appendix*, Fig. S2 *M* and *N*), consistent with the mRNA data (*SI Appendix*, Fig. S2 *E*). The levels of pNF-κB p65 were also significantly reduced by each treatment (*SI Appendix*, Fig. S2*O*), but none of them had any effect on pSTAT3 levels (*SI Appendix*, Fig. S2*P*). A single dose of etanercept was clearly insufficient to dampen STAT3 activation in ECTV-infected mice and is a likely reason why lung pathology was not reduced.

We assessed whether the mRNA and protein levels (*SI Appendix*, Fig. S2 *E–P*) of any of the factors correlated with the determinants of disease severity (weight loss, clinical scores, and histopathological scores). In the mock treatment group, IL-6, CCL2, CCL5, and CXCL10 mRNA levels (*SI Appendix*, Fig. S2 *F* and *J–L*) and sTNF and pSTAT3 protein levels (*SI Appendix*, Fig. S2 *N* and *P*) strongly positively correlated (Pearson's $r \geq 0.7$) with at least two of the determinants of disease severity (i.e., clinical and lung histopathological scores) (*SI Appendix*, Table S1). Expectedly, etanercept, cidofovir, and the combined treatment changed the correlation between levels of cytokines/cytokine-signaling pathways and disease severity to varying extents, with combined treatment having the most-significant effect. The combined treatment with only one dose of etanercept was clearly not sufficient to abolish positive correlations between weight loss and sTNF or weight loss and pSTAT3; however, it abrogated positive correlations between clinical scores and lung histopathological scores with all of the cytokines and cytokine-signaling pathways measured.

With the exception of a very small number of animals, it was evident that high levels of sTNF, pNF-κB p65, and pSTAT3 were expressed only in lungs of mice that lost the most weight (*SI Appendix*, Fig. S2*Q*). Notably, six (B2, B3, C1, C3, D1, and D3) out of eight animals highlighted in *SI Appendix*, Fig. S2*Q*, with significant weight losses at day 11 p.i., were the ones that exhibited early disease signs from day 6 p.i. Furthermore, the finding that high levels of sTNF correlated with disease severity is consistent with our previous report that sTNF is likely responsible for the pathology when produced in excess and that mTNF but not sTNF is necessary and sufficient to protect against excessive lung inflammation (6).

Combined Treatment with Cidofovir and Multiple Doses of Etanercept Protects from Lethal ECTV Infection. Antivirals are not effective in protecting against severe disease if treatment is initiated late after onset of disease signs. At that stage of the disease, tissue damage due to high viral load and excessive inflammation contribute to lung pathology, morbidity, and mortality. It was therefore important to determine whether the combined therapy would protect against a lethal dose of virus infection. Etanercept and/or cidofovir treatment were started at day 5 p.i. as mice infected with a lethal dose of ECTV exhibit clinical signs of disease as early as day 4 p.i. Etanercept and combined-treatment groups received additional doses of etanercept on day 7 and then daily from day 9 p.i. All surviving animals were euthanized on day 16 p.i. for various analyses.

Compared to the other treatment groups, weight loss and clinical signs were highly pronounced in mock-treated mice (Fig. 4 *A* and *B*), which succumbed by day 8 p.i. (Fig. 4*C*). Etanercept treatment had no effect on weight loss, and although it improved clinical scores significantly beginning at day 7, all animals died by day 9 p.i. Cidofovir and the combined treatment significantly reduced weight loss by day 8 p.i. and clinical scores as early as days 6 to 7 p.i. (Fig. 4 *A* and *B*). At day 16 when the experiment was terminated, four of the five animals in the cidofovir treatment group had succumbed to disease, whereas only one of the five animals in the combined-treatment group had died (Fig. 4*C*). Virus was below the limit of detection in the five surviving animals.

As the animals succumbed or were euthanized at different times (Fig. 4*A*), a comparison of the histopathological scores between the treatment groups is not possible. Nonetheless, lung pathology was more pronounced in mice that succumbed at earlier time points. Lung H&E sections revealed parenchymal edema and bronchial destruction in mock-treated mice (*SI Appendix*, Fig. S3 *A* and *B*). Treatment with etanercept alone reduced lung parenchymal edema (*SI Appendix*, Fig. S3 *C* and *D*), but it was not sufficient to protect mice from death. Cidofovir treatment had a modest effect in reducing edema and restored the bronchial epithelia (*SI Appendix*, Fig. S3 *E* and *F*). Expectedly, the combined-treatment group had the biggest reduction in lung pathology (*SI Appendix*, Fig. S3 *G* and *H*), but these animals were euthanized much later. The histopathological scores are shown in Fig. 4*D*.

While there were no significant changes in mRNA transcripts for many of the cytokines or chemokines between the treatment groups, with the exception of IL-12p40 and TGF- β, protein levels of pNF-κB p65 and pSTAT3 in the combined-treatment group were reduced significantly (Fig. 5 *A–L*). The one animal in the combined-treatment group that died on day 9 p.i. had received two doses of etanercept, whereas the remaining four animals that were euthanized on day 16 had been treated with etanercept nine times.

We conclude that multiple doses of etanercept in the combined therapy are more effective in protecting mice from an otherwise lethal infection through down-regulation of pNF-κB p65 and pSTAT3 levels.

Etanercept Mediates Inhibition of the NF-κB-Signaling Pathway via Reverse Signaling. Etanercept lessens lung pathology through reducing the bioavailability of sTNF, which is closely correlated with disease severity (*SI Appendix*, Table S1). In addition, etanercept can bind to mTNF on cells and potentially reverse signal to reduce inflammatory gene expression within those cells. We used bone marrow–derived macrophages (BMDMs) from triple mutant (TM) mice, which are engineered to express mTNF but not sTNF or TNFRI or TNFRII to determine the profile of inflammatory genes that were down-regulated by etanercept treatment through reverse signaling via mTNF. BMDMs were stimulated with lipopolysaccharide (LPS) to induce mTNF and proinflammatory mediators and then treated

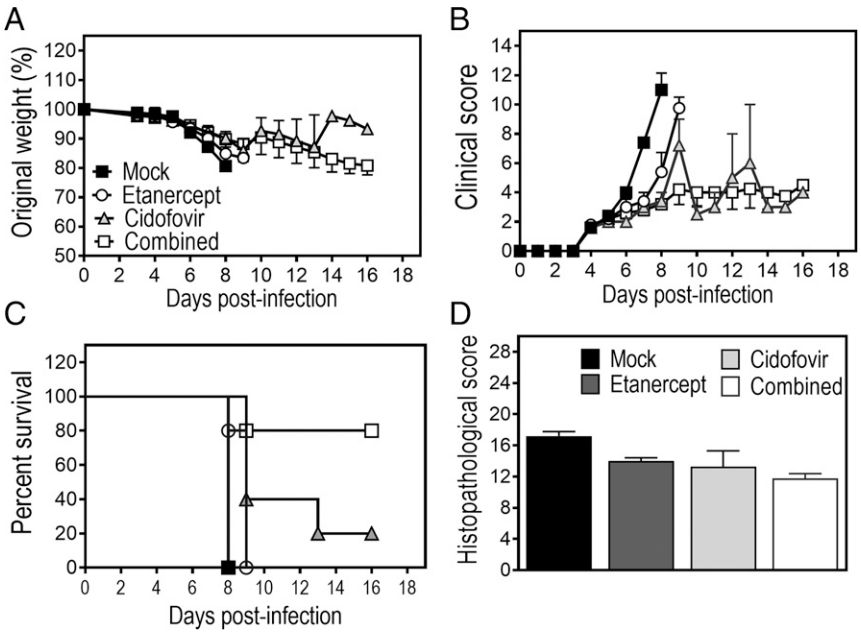

Fig. 4. Combined treatment with cidofovir and multiple doses of etanercept reduces weight loss, clinical disease, and lung pathology and protects mice from lethal ECTV infection. Groups of five WT mice were infected with 50 PFU ECTV (Naval) i.n. and were administered cidofovir (day 5 p.i.), multiple doses of etanercept (days 5 and 7 p.i. and daily from day 9 p.i.), or a combined treatment. Weight loss and clinical scores (*A* and *B*) were assessed until day 16 p.i. Animals with a clinical score of ≥10 and/or a body weight loss of ≥25% before the termination of experiment were euthanized on that day, while all remaining animals were euthanized on day 16 p.i. and lung tissue collected for various analyses. (*A* and *B*) Data were analyzed using two-way ANOVA with Sidak's multiple-comparisons tests. Survival data (*C*) were analyzed using log-rank (Mantel–Cox) test. The median survival time for mice treated with etanercept or cidofovir was 9 d, compared with a median survival of 8 d for mock-treated mice (log-rank test, mock versus etanercept, $P = 0.0088$; mock versus cidofovir, $P = 0.0016$). Survival for combined treated animals was 80% at the last time point (day 16 p.i.); hence, the median survival time was >16 d (log-rank test, $P = 0.0016$ relative to mock-treated mice). Histopathological scores (*D*) were derived from microscopic examination of the lung histology H&E sections. (*A*, *B*, and *D*). Data are expressed as means ± SEM.

with etanercept. The Mouse Signal Transduction Pathway Finder PCR array that screened for 84 genes was used (13). As reported previously, LPS treatment up-regulated 22 genes (13), and treatment with etanercept down-regulated four of those 22 genes significantly by more than twofold (*SI Appendix*, Table S2). These genes include *CCL2*, *SELP*, *NOS2*, and *PTGS2*, all of which play a central role in inflammatory responses, and their expression is regulated by the NF-κB pathway (23–26).

The most-common, prevalent form of NF-κB is a heterodimer of p50 or p52 subunit and the p65 subunit (27). The inactive form of NF-κB exists in the cytoplasm bound to the regulatory protein, inhibitor of NF-κB (IκB) (28). When activated via phosphorylation-induced, proteosome-mediated degradation of IκB, the NF-κB dimer is released and translocates to the nucleus (28). To gain further insights into the NF-κB-mediated mechanism(s) through which etanercept dampens inflammation, we used BMDMs from TM mice that were either left unstimulated or stimulated with LPS, treated with etanercept, and stained with a fluorescently labeled anti-NF-κB p65 antibody. As controls, BMDMs from $TNF^{-/-}$ mice were used. Unstimulated BMDM did not show any NF-κB p65–staining inside the nucleus, and diffuse red fluorescence (NF-κB p65) was only seen in the cytoplasm of cells (Fig. 5 *M* and *N*). LPS stimulation activated NF-κB p65, which translocated into the nucleus of BMDM from both strains of mice (Fig. 5 *O*, *P*, *S*, and *T*). Etanercept treatment (3 h or 6 h) markedly reduced translocation of NF-κB p65 to the nucleus in TM BMDM (Fig. 5 *Q* and *U*) but not in $TNF^{-/-}$ BMDM (Fig. 5 *R* and *V*).

The key mechanism for regulating NF-κB activation is through phosphorylation of IκB, which is mediated primarily by IκB kinase (IKK) (29). The IKK complex consists of two catalytic subunits, IKKα and IKKβ, and a regulatory subunit, IKKγ (30). Phosphorylated IKKα/β initiates IκB phosphorylation and degradation, thereby activating NF-κB (31). We determined the levels of phosphorylated IKKα/β following LPS stimulation and etanercept treatment of BMDMs from TM mice. LPS-induced phosphorylation/activation of IKKα/β was dramatically reduced by etanercept treatment (Fig. 5*W*). Taken together, our data indicates that the binding of etanercept to mTNF triggers reverse signaling and dampens inflammatory gene expression via inhibition of NF-κB activation and its nuclear translocation.

TM mice lack endogenous TNF-signaling like $TNF^{-/-}$ mice but will respond to etanercept due to mTNF expression, and the combined treatment should therefore be effective in TM mice. TM mice were infected with 25 PFU ECTV, and treatment was initiated at day 6 p.i. Animals were euthanized on day 8 p.i. due to morbidity in the mock-treated group.

Only etanercept treatment resulted in a significant reduction in weight loss at day 7 p.i., but by day 8, all treatment regimens were effective in reducing weight loss (Fig. 6*A*). TM mice given the combined treatment had the lowest clinical scores, whereas monotherapy with etanercept or cidofovir resulted in significant improvements in clinical scores compared to the mock-treated group (Fig. 6*B*).

Cidofovir, either alone or in combination with etanercept, resulted in substantially lower lung viral load compared to mock- or etanercept-treated mice (Fig. 6*C*). Viral load in mock-treated and etanercept-treated animals were comparable.

Etanercept or cidofovir treatment decreased histopathological scores compared to the mock-treated group (Fig. 6*D*). Histopathological scores are based on microscopic examination of lung H&E sections, shown in Fig. 6 *E–L*. The different treatment regimens reduced lung pathology, similar to observations made in WT mice (Fig. 3 *A–H*). The data are consistent with etanercept reducing lung pathology dampening cytokine and chemokine responses via reverse signaling through mTNF.

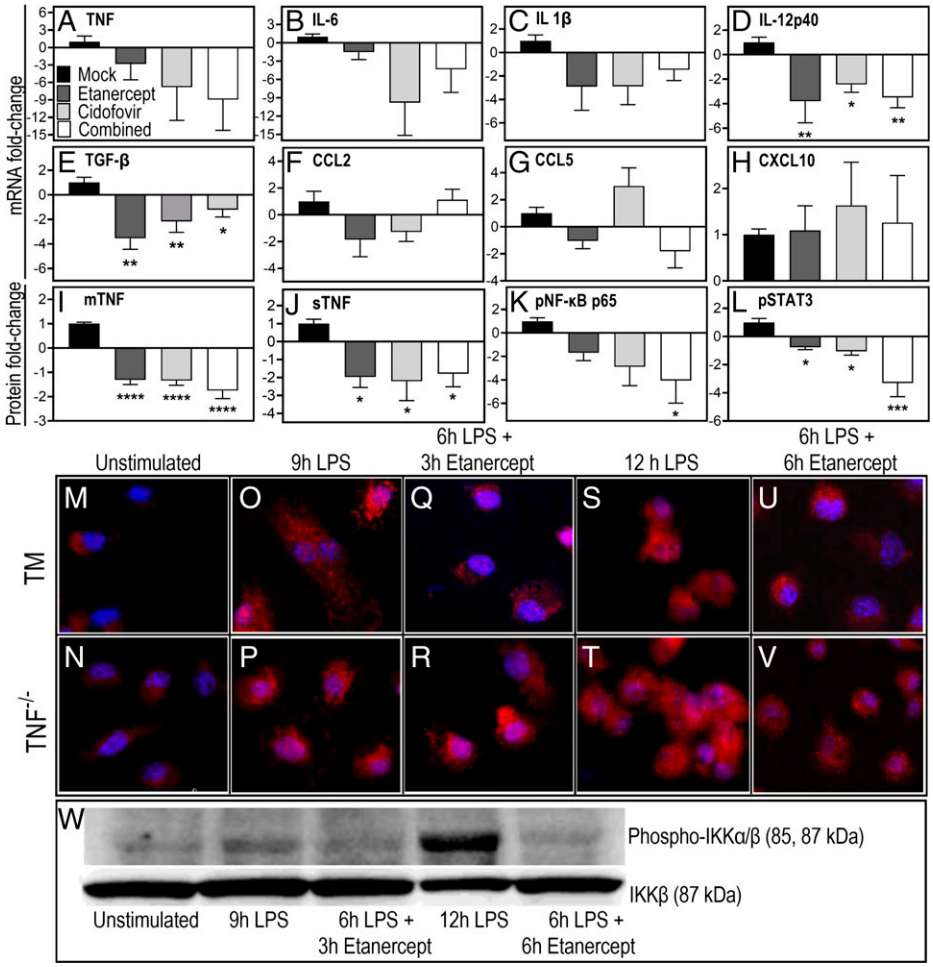

Fig. 5. Combined treatment with cidofovir and multiple doses of etanercept reduces cytokine production and activation of NF-κB and STAT3 pathways. Lung tissue sections were obtained from mice that were infected and treated as described in Fig. 4. Levels of mRNA transcripts for cytokines and chemokines were determined using qPCR (*A*–*H*), and protein levels of mTNF (*I*), sTNF (*J*) pNF-κB p65 (*K*), and pSTAT3 (*L*) were measured using Western blotting. Western blot data were quantified by densitometry and levels of β-actin were used as loading control. Data are expressed as mean fold-change relative to mock-treated group ± SEM and were analyzed using one-way ANOVA with Holm–Sidak's multiple-comparisons tests. $*P < 0.05$; $**P < 0.01$; $***P < 0.001$; and $****P < 0.0001$. (*M*–*V*) Etanercept treatment inhibits LPS-induced nuclear localization of NF-κB p65 and IKKα/β phosphorylation. BMDM from TM (mTNF$^{\Delta/\Delta}$.TNFRI$^{-/-}$.II$^{-/-}$) or TNF$^{-/-}$ mice were grown on sterile coverslips and left unstimulated (*M* and *N*), stimulated with LPS for 9 h (*O* and *P*), or stimulated with LPS for 6 h after which they were treated with etanercept at 10 μg/mL for 3 h in the presence of LPS (*Q* and *R*). Separate populations of cells were treated with LPS for 12 h (*S* and *T*) or treated with LPS for 6 h and then with etanercept at 10 μg/mL for a further 6 h in the presence of LPS (*U* and *V*). Cells were then fixed with 4% paraformaldehyde and stained with primary goat anti-mouse polyclonal NF-κB p65 antibody and followed by secondary goat anti-rabbit IgG Alexa Fluor 546 (red) to visualize under the fluorescence microscope. For visualization of nucleus, cells were counterstained with DAPI (blue). Translocation of NF-κB p65 is seen as pink fluorescence in the nucleus. Slides were examined at 1,000× magnification. (*W*) Treated BMDM from TM mice were harvested for isolation of total proteins, and levels of phosphorylated IKKα/β and IKKβ were measured by Western blotting.

Combined Treatment with Cidofovir and S3I-201 Reduces Viral Load and Lung Pathology and Ameliorates Clinical Disease Severity during ECTV Infection. The preceding data established that combined treatment with cidofovir and multiple doses of etanercept was most effective in dampening inflammation and protecting mice from an otherwise lethal infection via inhibition of the NF-κB- and STAT3-signaling pathways. The STAT3 pathway is downstream of the NF-κB pathway, and dysregulated TNF levels (excessive or deficient) dysregulate the NF-κB pathway and hyperactivate STAT3, causing severe pneumonia during ECTV infection (6, 13). We have previously shown that inhibition of STAT3 activation with a selective inhibitor, S3I-201, significantly reduced lung inflammation and pathology but was not sufficient to protect the animals from death (6). We reasoned that combined treatment with cidofovir and S3I-201 might be effective in reducing morbidity and mortality in ECTV-infected WT and TNF$^{-/-}$ mice.

Groups of WT and TNF$^{-/-}$ mice were infected with a lethal dose of ECTV and treated with S3I-201, cidofovir, or both drugs at day 7 p.i. The relevant groups were treated with S3I-201 again on day 8, and mice were euthanized on day 9 p.i. Just 1 d after treatment initiation, S3I-201 treatment resulted in significant reductions in clinical scores (Fig. 7 *A* and *B*), with the biggest reduction observed in the combined-treatment groups, particularly in TNF$^{-/-}$ mice. Cidofovir treatment reduced clinical scores between days 8 and 9 in both strains of mice (Fig. 7 *A* and *B*). Cidofovir or combined treatment reduced the lung viral load, but S3I-201 had no effect (Fig. 7*C*). Based on histopathological scores, both S3I-201 and combined treatment were equally effective in reducing lung pathology in both WT and TNF$^{-/-}$ mice (Fig. 7*D*), mainly due to the reduction of parenchymal edema (*SI Appendix*, Fig. S4).

To understand the mechanism(s) through which the combined treatment ameliorated lung pathology, we measured the

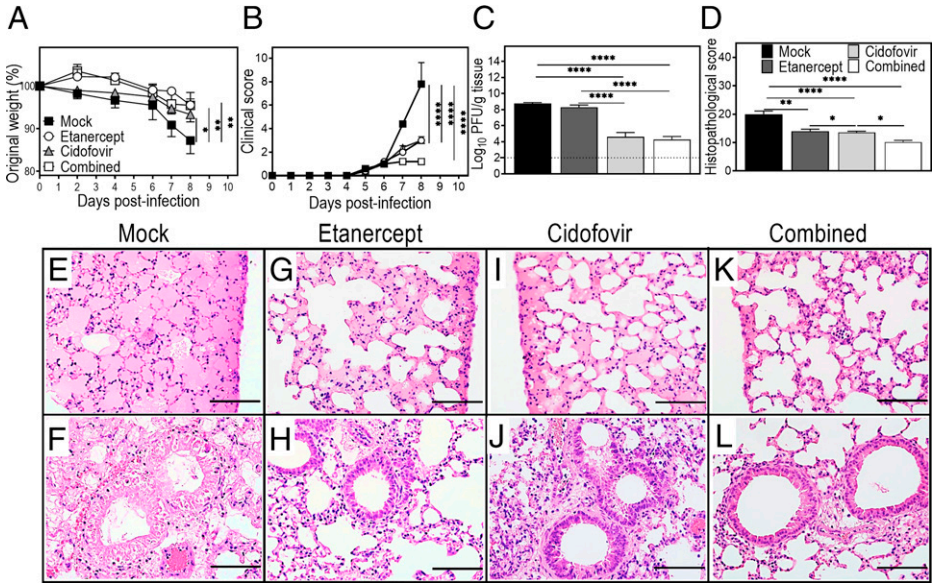

Fig. 6. Etanercept reduces weight loss, clinical scores, and lung histopathological scores in ECTV-infected TM mice through reverse signaling. Groups of five TM mice were infected with 25 PFU of ECTV (Naval) i.n. Animals were treated with etanercept or cidofovir or both drugs (combined) on day 6 p.i. and euthanized on day 8 p.i. due to high morbidity in the mock-treated group. Weights (*A*) and clinical scores (*B*) were monitored during the course of infection. Data were analyzed using two-way ANOVA with Sidak's posttests. Viral load data were log transformed (*C*) and analyzed using ordinary one-way ANOVA followed by uncorrected Fisher's LSD post hoc tests. Histopathological scores (*D*) were generated based on microscopic examination of lung H&E sections (*E–L*), and statistical analysis was done using ordinary one-way ANOVA followed by Tukey's post hoc tests. Data are expressed as means ± SEM $*P < 0.05$; $**P < 0.01$; and $****P < 0.0001$. The broken line in *C* corresponds to the limit of virus detection.

fold changes in mRNA transcripts and proteins for some proinflammatory cytokines, chemokines, and cytokine-signaling pathways (*SI Appendix*, Fig. S5 *A–L*). S3I-201 or the combined treatment significantly down-regulated mRNA levels of IL-1β, TGF-β, and CCL5, but only the latter reduced levels of mRNA transcripts for TNF, IL-12p40, CCL2, and CXCL10.

None of the treatment regiments affected mTNF, sTNF, or NF-κB p65 levels (*SI Appendix*, Fig. S5 *I–K*), suggesting that inhibition of STAT3 activation might not affect the NF-κB pathway. The determinants of disease severity during respiratory ECTV infection significantly correlated with sTNF and pSTAT3 protein levels (*SI Appendix*, Table S1), but neither S3I-201 nor cidofovir treatment had any significant effects on sTNF levels (*SI Appendix*, Fig. S5*J*). In contrast, levels of pSTAT3 protein were reduced by all three treatment regimens compared to mock treatment (*SI Appendix*, Fig. S5*L*). The decrease in STAT3 activation in S3I-201 or combined-treatment groups was consistent with reduced lung histopathological scores, but that was not the case with cidofovir treatment.

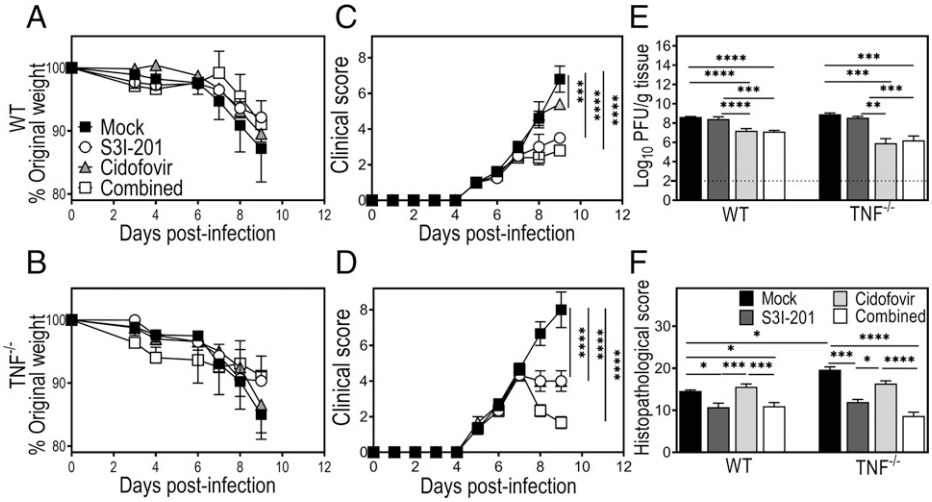

Fig. 7. Combined treatment with S3I-201 and cidofovir reduces clinical scores, histopathological scores, and lung viral load during ECTV infection. Age-matched groups of female WT mice ($n = 4$ or 5) and TNF$^{-/-}$ mice ($n = 3$) were infected with 75 PFU ECTV (Moscow) i.n. Mice were treated with cidofovir (day 7 p.i.) or STAT3 inhibitor (days 7 and 8 p.i.) or both drugs (combined). Mice were monitored for disease severity; weight loss (*A* and *B*) and clinical scores (*C* and *D*), euthanized at day 9 p.i. and lung viral load (*E*) and histopathological scores (*F*) were determined. (*A–D*) Data were analyzed using two-way ANOVA followed by Sidak's post hoc tests compared to the means of mock-treated group. (*E*) Viral load data were log transformed and analyzed using ordinary one-way ANOVA followed by uncorrected Fisher's LSD post hoc tests. Microscopic examination of lung H&E sections were used to generate histopathological scores (*F*), and statistical analysis was done using ordinary one-way ANOVA followed by Tukey's post hoc tests. Data are expressed as means ± SEM $*P < 0.05$; $**P < 0.01$; $***P < 0.001$; and $****P < 0.0001$. The broken line in *E* corresponds to the limit of virus detection.

Taken together, it is likely that reduced levels of pSTAT3, in addition to TNF, IL-12p40, CCL2, CXCL10, and possibly IL-1β, TGF-β, and/or CCL5 contributed to the reduction in lung pathology in the combined-treatment regimen using cidofovir and SI-301.

Discussion

Viral pneumonia is a leading but underestimated cause of deaths worldwide (32). There are no specific treatments for this condition. In this study, we have addressed two interrelated key questions. The first relates to the development of an effective treatment for viral pneumonia. The second pertains to why antivirals are ineffective in reducing morbidity and mortality if treatment is initiated late after the onset of disease symptoms.

Uncontrolled virus replication in the lung has deleterious cytopathic effects resulting in lung injury, and treatment with an antiviral is pivotal in controlling virus replication, which in turn might ameliorate lung pathology. However, treatment with antiviral alone is not sufficient to protect against severe pneumonia caused by viral infection, particularly when the treatment is delayed. For example, in individuals infected with IAV, the neuraminidase inhibitor oseltamivir is effective only when treatment is commenced within 48 h of onset of symptoms (33, 34). Similarly, the antiviral efficacy of valaciclovir against varicella zoster virus, the causative agent of herpes zoster, is dramatically reduced when administered after 72 h of rash onset (35). The efficacy of cidofovir has been evaluated in mouse models of OPXV infection, including vaccinia virus, cowpox virus, and ECTV (36–38). Cidofovir was effective when treatment was initiated at 3 d p.i. but was only partially protective if administered after that time period (36–38).

Viral replication in the early stages of infection triggers an inflammatory response driving the production of cytokines and chemokines, which are consistently associated with the severity of infection, including IAV and SARS-CoV-2 infection (39, 40) in humans and ECTV in mice (6, 13). We posited that the reason for ineffectiveness of antivirals to reduce morbidity or mortality late after onset of disease symptoms is due to lung pathology caused by an exuberant inflammatory response in addition to pathology and tissue damage caused by the replicating virus. Using a respiratory OPXV pneumonia model, we have established proof of concept that viral pneumonia can be treated effectively through simultaneous targeting of both virus and inflammation. We have used two anti-inflammatory drugs targeting two different cytokine-signaling pathways to demonstrate that an antiviral drug can be used to treat pneumonia effectively, even when the treatment initiation is delayed after the onset of disease signs if inflammation is also dampened.

We initially focused on TNF as it is one of the earliest inflammatory cytokines to be produced following viral infection and is known to be associated with driving lung inflammation, severe pathology, and death during respiratory viral infections (6, 11, 41, 42). Anti-TNF therapeutics have been used to treat several chronic inflammatory conditions such as rheumatoid arthritis, inflammatory bowel disease, and ankylosing spondylitis (43, 44). However, in contrast to chronic inflammatory diseases that require etanercept administration once or twice a week, our results indicated that multiple doses of etanercept were required to effectively treat viral pneumonia in the combined therapy. It is likely that levels of TNF produced during an acute respiratory viral infection might be different to those during chronic inflammatory diseases, and as a consequence, multiple doses of etanercept are required.

The combined treatment with etanercept and cidofovir effectively dampened lung inflammation and significantly reduced loss in body weight, disease severity, and lung pathology and protected mice from an otherwise lethal infection. Our data indicates that combined treatment down-regulated levels of inflammatory cytokines and chemokines, namely TNF, IL-6, IL-1β, IL-12p40, TGF-β, and CCL5 (Fig. 5 and *SI Appendix*, Fig. S2). Most of these cytokines are known to cause lung pathology during respiratory ECTV infection when produced in excess (6, 13). Combined treatment reduced recruitment of inflammatory monocytes to the lung. These myeloid cells migrate to the lung by responding to CCL2 through CCR2 expression and produce inflammatory cytokines like IL-1, TNF, IL-6, CCL2, and CXCL10 (45). Sustained elevation of TNF, IL-1, IL-6, and IL-8 have been associated with poor clinical outcomes in patients with acute respiratory distress syndrome (46). TGF-β, IL-12p40, and CCL5 can contribute to lung injury through development of pulmonary edema, fibrosis, and recruitment of neutrophils, respectively (47–49). Consistent with our results, previous studies have also shown reductions in levels of these inflammatory mediators through TNF blockade, indicating the potential use of this therapy in controlling hypercytokinemia-associated lung disease, including viral pneumonia (50–52). Anti-TNF treatment has been found to reduce cytokine production and lung pathology in mice infected with RSV or IAV (53–55), and there have been suggestions to repurposing of anti-TNF therapy for treatment of coronavirus disease 19 (COVID-19) (11).

TNF-signaling triggers an inflammatory cascade through activation of the NF-κB pathway (56). Etanercept treatment reduced NF-κB activation in vitro and in vivo and consequently reduced levels of expression of inflammatory genes regulated by this pathway. Etanercept interacts with mTNF and, through reverse signaling, inhibited the phosphorylation of IKKα/β and the translocation of NF-κB p65 to the nucleus.

STAT3 is an important transcription factor that is crucial for induction of a number of proinflammatory and immune response genes (57). The NF-κB pathway regulates STAT3-signaling, mainly through the production of IL-6 or suppressor of cytokine signaling 3, which enhances or represses STAT3 activation, respectively (57, 58). We have found that up-regulated levels of pSTAT3 in the lungs of ECTV-infected mice strongly correlated with disease severity, consistent with our previous report (6). Etanercept-induced reduction in pSTAT3 levels in the combined-treatment regimen with cidofovir also strongly correlated with reduced loss in body weights, disease severity, and lung pathology in ECTV-infected mice. That finding suggested that targeting STAT3 to reduce inflammation might also be effective in the combined anti-inflammatory drug plus antiviral treatment. Indeed, combined treatment with S3I-201 and cidofovir reduced the clinical signs and lung pathology and was associated with diminished levels of TNF, IL-1β, IL-12p40, TGF-β, CCL2, CCL5, and CXCL10 mRNA.

Interestingly, in both the combined regimens of treatment (i.e., etanercept plus cidofovir and S3I-201 plus cidofovir), a common set of cytokines and chemokines, namely TNF, IL-1β, IL12p40, TGF-β, and CCL5, were down-regulated. It is tempting to speculate that some if not all of these factors may have contributed to disease severity and lung pathology during pneumonia caused by ECTV infection. However, our results indicate that targeting just one cytokine (TNF) or a transcription factor (STAT3) is sufficient to ameliorate lung pathology. It is known that the different signaling pathways activated by the cytokines listed here can cross-regulate each other and that dysregulated production of one cytokine can dysregulate other cytokine-signaling pathways (6, 13).

It is of significance that S3I-201 was effective in dampening lung inflammation in ECTV-infected $TNF^{-/-}$ mice in which STAT3 is dysregulated and hyperphosphorylated (6). Inhibition of STAT3 to dampen lung inflammation will be more appropriate in individuals who cannot be treated with etanercept due to

contraindications or when TNF may not be the driver of lung inflammation, and thus, an alternative anti-inflammatory drug would be necessary for the combined therapy.

Our results are in agreement with several other studies which have reported that combined treatment with an antiviral and anti-inflammatory drug to be superior to antiviral alone in providing protection against viral pneumonia. Recently, Kalil et al. showed that combined treatment with baricitinib, a selective inhibitor of Janus kinase and remdesivir (an inhibitor of viral, RNA-dependent RNA polymerase) had a greater impact than remdesivir alone in reducing recovery time and improving clinical status of patients hospitalized with COVID-19 (59). Similarly, different combined-treatment approaches, at least in mouse models, have been reported as promising therapeutic options against influenza pneumonia, namely, hepatocyte growth factor and oseltamivir (60), clopidogrel (platelet receptor antagonist) and oseltamivir (61), 1,8-cineol and oseltamivir (62), L-N^G-monomethyl-arginine and oseltamivir (63), and sphingosine-1-phosphate receptor agonist and oseltamivir (64). However, translation of these animal studies into clinical practice is limited, as treatments in these studies were commenced either on the day of viral infection or before the onset of clinical signs. Generally, patients present to a hospital or seek medical advice after the onset of symptoms, once they have developed pneumonia. Our study has addressed this gap in treatment strategy by demonstrating that the administration of antiviral and anti-inflammatory drugs after onset of symptoms is effective in treating viral pneumonia. This is a realistic time frame, as it more closely reflects time frames when patients present at hospitals.

The use of TNF inhibitors to treat chronic inflammatory conditions over extended periods is linked with immunosuppression and increased risk for secondary infections or reactivation of latent infections, especially tuberculosis and viral hepatitis caused by *Mycobacterium tuberculosis* and hepatitis B and C virus, respectively (65, 66). However, what we are proposing is short-term treatment with an anti-TNF agent to treat viral pneumonia. At the time that these animal experiments were initiated, tecovirimat (ST-246), an antiviral developed specifically for OPXV (67), had not been approved by the US Food and Drug Administration. Tecovirimat was developed and now stockpiled in the US Strategic National Stockpile to counter any potential OPXV-based bioterror attack. We opted to use cidofovir solely to establish proof of concept that targeting both virus and inflammation late after disease onset following respiratory infection would be more effective in effectively treating viral pneumonia. Tecovirimat has been shown to be effective against all of the OPXV tested, but the efficacy of this drug is significantly reduced when treatment is delayed (68). It would therefore be desirable to test the efficacy of tecovirimat in the combined-treatment approach against ECTV.

We initiated treatment in all animal groups 1 to 2 d post onset of disease signs in at least some animals to compare the treatment regimes' efficacy and undertake statistical analysis. Even though animals were infected with comparable doses of the virus, they started losing weight and showed disease signs at different times, even within the same treatment group. We had expected such findings in our animal experiments. However, in applying the combined therapy to treating viral pneumonia in humans, each patient will need to be assessed individually and given monotherapy or combined therapy, depending on the timing of their presentation to a hospital.

In summary, delayed treatment with etanercept plus cidofovir during respiratory ECTV infection after the onset of disease signs effectively reduced clinical signs, improved lung pathology, and protected mice from death. These beneficial effects are mediated through reduced lung viral load as well as diminished expression of proinflammatory cytokines and their signaling pathways, in particular the NF-κB- and STAT3-signaling pathways. This work supports the idea that the combined-treatment approach may be applicable to treatment of pneumonia caused by other important viruses, including seasonal and pandemic IAV and SARS-CoV-2 (58, 69).

Materials and Methods

Animal Studies. Animal experiments were performed in accordance with protocols approved by the Animal Ethics Committee of the University of Tasmania (UTAS) (Protocol no. A0016372) and the Animal Ethics and Experimentation Committee of the Australian National University (ANU) (Protocol nos. A2011/011 and A2014/018). Specific pathogen–free, 6- to 12-wk-old female mice on a C57BL/6J background were obtained from the Australian Phenomics Facility, ANU, Canberra, the Cambridge Farm Facility, UTAS, Tasmania, and the Animal Resource Centre, Western Australia, Australia. $TNF^{-/-}$ mice (70) and a TM expressing only mTNF but lacking sTNF, TNFRI, and TNFRII (TM or $mTNF^{\Delta/\Delta}$.$TNFRI^{-/-}$.$II^{-/-}$) (13) were used in the animal experiments.

Cell Lines, BMDMs, and Viruses. BS-C-1 cells (ATCC No. CCL-26) were cultured in Eagle's minimum essential medium supplemented with 2 mM L-glutamine (Sigma-Aldrich), antibiotics (penicillin, 50 U/mL; streptomycin, 50 μg/mL; and neomycin, 100 μg/mL) (Sigma-Aldrich), 1 mM 4-(2-hydroxyethyl)-1-piperazineethanesulfonic acid (HEPES) (Invitrogen), and 10% heat inactivated fetal bovine serum (FBS) as described in detail elsewhere (13).

BMDMs were generated from TM and $TNF^{-/-}$ mice as previously described (13). Cells were cultured in Dulbecco's modified Eagle medium/F-12, supplemented with 10% FBS and 10% L929-cell conditioned medium (13).

The Naval (71) and Moscow (ATCC No. VR-1374) ECTV strains were propagated in BS-C-1 cells and quantified using viral plaque assay as previously described (72). For more information, refer to *SI Appendix, Materials and Methods*. Both strains of virus have minor genetic differences and exhibit similar degrees of virulence in BALB/c WT, C57BL/6 WT, and C57BL/6 $TNF^{-/-}$mice (13, 73). The Naval and Moscow virus strains were used to establish that the combined treatment was equally effective against both strains at sublethal and lethal doses.

Plaque Assay for Virus Quantification. Viral titers in tissues were determined as virus PFU per milliliter of homogenized tissue samples using a plaque assay, previously described elsewhere (72). For details, refer to *SI Appendix, Materials and Methods*.

Virus Infection, Animal Weights, Clinical Scores, and Treatments. Mice were anesthetized and infected i.n. with ECTV Moscow or Naval strains in 30 μL PBS. Virus dose used to infect mice was confirmed by back-titrating serial dilutions of the inoculum on the same day. Some groups of mice were administered intraperitoneally with the following drugs after the onset of disease signs: cidofovir (Vistide; Gilead Sciences Inc.) at 100 mg/kg, etanercept (Enbrel; Pfizer Inc.) at 2.5 mg/kg, or S3I-201 (STAT3 inhibitor VI, Sigma-Aldrich, catalog no. 573102) at 5 mg/kg. For full details, refer to *SI Appendix, Materials and Methods*. For ethical reasons, mice that were severely moribund with a clinical score of ≥10 and/or a body weight loss of ≥20% (UTAS) or 25% (ANU) were euthanized, tissues collected for analysis, and mice considered dead the following day.

Histopathological Examination of Lung Tissue. H&E-stained lung sections were assessed for histopathology using a semiquantitative scoring system as described previously (6). For more details, refer to *SI Appendix, Materials and Methods*.

RNA Extraction, Complimentary DNA Generation, and qRT-PCR. Total RNA from the lung tissue was extracted using TRIzol reagent (Thermo Fisher Scientific, catalog no. 15596026), and complimentary DNA (cDNA) was synthesized using RevertAid first-strand cDNA synthesis kit (Thermo Fisher Scientific, catalog no. K1622). mRNA expression levels of selected cytokines and chemokines were then measured using qRT-PCR. Details on quantitation of cytokine/chemokine mRNA, including RNA extraction and cDNA generation, are presented in *SI Appendix, Materials and Methods*.

Protein Extraction and Western Blot Analysis. The lung tissue was homogenized and lysed for the total protein extraction. A total of 25 μg protein was resolved by sodium dodecyl sulfate–polyacrylamide gel electrophoresis, which was then transferred to polyvinylidene fluoride membrane using an iBlot 2 gel transfer device (Thermo Fisher Scientific). The immunoblot was stained with the selected primary/secondary antibodies for quantifying protein expression levels of sTNF/mTNF (Santa Cruz Biotechnology, catalog no. sc-12744), pNF-κB p65 (Ser536) (Thermo Fisher Scientific, catalog no. MA5-15160), pIKKα/β (Ser176/180) (Cell Signaling Technology, catalog no. 2697), and

pSTAT3 (Tyr705) (Cell Signaling Technology, catalog no. 9145). Finally, the blot was developed using SuperSignal West Pico PLUS chemiluminescent substrate (Thermo Fisher Scientific, catalog no. 34580), visualized in a chemiluminescent imager (Amersham 600, Cytiva Life Sciences), and protein bands were quantified with the ImageJ software as described elsewhere (74). Details on the procedure and antibodies used are included in *SI Appendix, Materials and Methods*.

Flow Cytometric Analysis of Lung Immune Cells. Lung tissue samples were digested with DNase I and collagenase, and flow cytometry of lung leukocytes was undertaken as described previously (6). For details, refer to *SI Appendix, Materials and Methods*.

Immunocytochemistry. BMDMs generated from TM and TNF$^{-/-}$ mice were fixed with 4% paraformaldehyde and permeabilized 0.25% Triton X-100. The fixed cells were then stained with anti-NF-κB p65 antibody followed by counter staining with DAPI to determine the nuclear translocation of NF-κB p65. Details on the procedure are included in *SI Appendix, Materials and Methods*.

Statistical Analysis. Statistical analyses of experimental data, as indicated in the legend to each figure, were performed using appropriate tests to compare results using GraphPad Prism 9 (GraphPad Software, Inc.). A value of $P < 0.05$ was taken to be significant: $^{*}P \leq 0.05$; $^{**}P \leq 0.01$; $^{***}P \leq 0.001$; and $^{****}P \leq 0.0001$.

Data Availability. All study data are included in the article and/or *SI Appendix*.

ACKNOWLEDGMENTS. This work was supported by grants from the National Health and Medical Research Council of Australia (Grant 1007980) and the Medical Protection Society of Tasmania Inc., Tasmania, Australia. The funders had no role in study design, data collection and interpretation, or the decision to submit the work for publication. We gratefully acknowledge Prof. Jane Dahlstrom, Canberra Hospital for helping us develop the lung histopathology scoring system and Prof. Antonio Alcamí, Centro de Biología Molecular Severo Ochoa, Madrid for the gift of the Naval strain of ECTV. We thank the UTAS Animal Services Division and the ANU Phenomics Facility for the care and breeding of mice. P.P. was the recipient of a Tasmanian School of Medicine Research Scholarship through the UTAS.

1. P. J. Ross, A. Seaton, H. M. Foreman, W. H. Morris Evans, Pulmonary calcification following smallpox handler's lung. *Thorax* **29**, 659–665 (1974).
2. L. P. Tavares, M. M. Teixeira, C. C. Garcia, The inflammatory response triggered by Influenza virus: A two edged sword. *Inflamm. Res.* **66**, 283–302 (2017).
3. P. Pandey, G. Karupiah, Targeting tumour necrosis factor to ameliorate viral pneumonia. *FEBS J.*, 10.1111/febs.15782 (2021).
4. R. Alon *et al.*, Leukocyte trafficking to the lungs and beyond: Lessons from influenza for COVID-19. *Nat. Rev. Immunol.* **21**, 49–64 (2021).
5. M. M. Stanford, G. McFadden, G. Karupiah, G. Chaudhri, Immunopathogenesis of poxvirus infections: Forecasting the impending storm. *Immunol. Cell Biol.* **85**, 93–102 (2007).
6. M. J. Tuazon Kels *et al.*, TNF deficiency dysregulates inflammatory cytokine production, leading to lung pathology and death during respiratory poxvirus infection. *Proc. Natl. Acad. Sci. U.S.A.* **117**, 15935–15946 (2020).
7. J. Wang *et al.*, Anti-inflammatory effects of apigenin in lipopolysaccharide-induced inflammatory in acute lung injury by suppressing COX-2 and NF-kB pathway. *Inflammation* **37**, 2085–2090 (2014).
8. A. J. Vogel, S. Harris, N. Marsteller, S. A. Condon, D. M. Brown, Early cytokine dysregulation and viral replication are associated with mortality during lethal influenza infection. *Viral Immunol.* **27**, 214–224 (2014).
9. R. L. Peper, H. Van Campen, Tumor necrosis factor as a mediator of inflammation in influenza A viral pneumonia. *Microb. Pathog.* **19**, 175–183 (1995).
10. A. Alejo *et al.*, A chemokine-binding domain in the tumor necrosis factor receptor from variola (smallpox) virus. *Proc. Natl. Acad. Sci. U.S.A.* **103**, 5995–6000 (2006).
11. P. C. Robinson, D. Richards, H. L. Tanner, M. Feldmann, Accumulating evidence suggests anti-TNF therapy needs to be given trial priority in COVID-19 treatment. *Lancet Rheumatol.* **2**, e653–e655 (2020).
12. B. Puthothu *et al.*, Association of TNF-alpha with severe respiratory syncytial virus infection and bronchial asthma. *Pediatr. Allergy Immunol.* **20**, 157–163 (2009).
13. Z. Al Rumaih *et al.*, Poxvirus-encoded TNF receptor homolog dampens inflammation and protects from uncontrolled lung pathology during respiratory infection. *Proc. Natl. Acad. Sci. U.S.A.* **117**, 26885–26894 (2020).
14. R. A. Black *et al.*, A metalloproteinase disintegrin that releases tumour-necrosis factor-α from cells. *Nature* **385**, 729–733 (1997).
15. Z. Ji, L. He, A. Regev, K. Struhl, Inflammatory regulatory network mediated by the joint action of NF-kB, STAT3, and AP-1 factors is involved in many human cancers. *Proc. Natl. Acad. Sci. U.S.A.* **116**, 9453–9462 (2019).
16. S. I. Grivennikov, M. Karin, Dangerous liaisons: STAT3 and NF-kappaB collaboration and crosstalk in cancer. *Cytokine Growth Factor Rev.* **21**, 11–19 (2010).
17. M.-C. Park *et al.*, Long-term efficacy, safety and immunogenicity in patients with rheumatoid arthritis continuing on an etanercept biosimilar (LBEC0101) or switching from reference etanercept to LBEC0101: An open-label extension of a phase III multicentre, randomised, double-blind, parallel-group study. *Arthritis Res. Ther.* **21**, 122 (2019).
18. P. Cole, X. Rabasseda, The soluble tumor necrosis factor receptor etanercept: A new strategy for the treatment of autoimmune rheumatic disease. *Drugs Today (Barc)* **40**, 281–324 (2004).
19. M. E. Weinblatt *et al.*, Efficacy and safety of etanercept 50 mg twice a week in patients with rheumatoid arthritis who had a suboptimal response to etanercept 50 mg once a week: Results of a multicenter, randomized, double-blind, active drug-controlled study. *Arthritis Rheum.* **58**, 1921–1930 (2008).
20. U. Meusch, M. Rossol, C. Baerwald, S. Hauschildt, U. Wagner, Outside-to-inside signaling through transmembrane tumor necrosis factor reverses pathologic interleukin-1β production and deficient apoptosis of rheumatoid arthritis monocytes. *Arthritis Rheum.* **60**, 2612–2621 (2009).
21. A. Pallai *et al.*, Transmembrane TNF-α reverse signaling inhibits lipopolysaccharide-induced proinflammatory cytokine formation in macrophages by inducing TGF-β: Therapeutic implications. *J. Immunol.* **196**, 1146–1157 (2016).
22. J. M. Bathon *et al.*, A comparison of etanercept and methotrexate in patients with early rheumatoid arthritis. *N. Engl. J. Med.* **343**, 1586–1593 (2000).
23. J. Pan, L. Xia, L. Yao, R. P. McEver, Tumor necrosis factor-alpha- or lipopolysaccharide-induced expression of the murine P-selectin gene in endothelial cells involves novel kappaB sites and a variant activating transcription factor/cAMP response element. *J. Biol. Chem.* **273**, 10068–10077 (1998).
24. X. Deng *et al.*, Transcriptional regulation of increased CCL2 expression in pulmonary fibrosis involves nuclear factor-κB and activator protein-1. *Int. J. Biochem. Cell Biol.* **45**, 1366–1376 (2013).
25. D. Arias-Salvatierra, E. K. Silbergeld, L. C. Acosta-Saavedra, E. S. Calderon-Aranda, Role of nitric oxide produced by iNOS through NF-κB pathway in migration of cerebellar granule neurons induced by Lipopolysaccharide. *Cell. Signal.* **23**, 425–435 (2011).
26. P. P. Tak, G. S. Firestein, NF-kappaB: A key role in inflammatory diseases. *J. Clin. Invest.* **107**, 7–11 (2001).
27. F. Chen, V. Castranova, X. Shi, L. M. Demers, New insights into the role of nuclear factor-kappaB, a ubiquitous transcription factor in the initiation of diseases. *Clin. Chem.* **45**, 7–17 (1999).
28. A. Oeckinghaus, S. Ghosh, The NF-kappaB family of transcription factors and its regulation. *Cold Spring Harb. Perspect. Biol.* **1**, a000034 (2009).
29. T. Liu, L. Zhang, D. Joo, S. C. Sun, NF-κB signaling in inflammation. *Signal Transduct. Target. Ther.* **2**, 17023 (2017).
30. S. C. Sun, S. C. Ley, New insights into NF-kappaB regulation and function. *Trends Immunol.* **29**, 469–478 (2008).
31. Z. Chen *et al.*, Signal-induced site-specific phosphorylation targets I kappa B alpha to the ubiquitin-proteasome pathway. *Genes Dev.* **9**, 1586–1597 (1995).
32. O. Ruuskanen, E. Lahti, L. C. Jennings, D. R. Murdoch, Viral pneumonia. *Lancet* **377**, 1264–1275 (2011).
33. T. Jefferson *et al.*, Neuraminidase inhibitors for preventing and treating influenza in adults and children. *Cochrane Database Syst. Rev.* **4**, CD008965 (2014).
34. L. Dou *et al.*, Decreased hospital length of stay with early administration of oseltamivir in patients hospitalized with influenza. *Mayo Clin. Proc. Innov. Qual. Outcomes* **4**, 176–182 (2020).
35. D. Ormrod, K. Goa, Valaciclovir: A review of its use in the management of herpes zoster. *Drugs* **59**, 1317–1340 (2000).
36. D. C. Quenelle, D. J. Collins, E. R. Kern, Efficacy of multiple- or single-dose cidofovir against vaccinia and cowpox virus infections in mice. *Antimicrob. Agents Chemother.* **47**, 3275–3280 (2003).
37. D. F. Smee, K. W. Bailey, M. H. Wong, R. W. Sidwell, Effects of cidofovir on the pathogenesis of a lethal vaccinia virus respiratory infection in mice. *Antiviral Res.* **52**, 55–62 (2001).
38. M. Bray *et al.*, Cidofovir protects mice against lethal aerosol or intranasal cowpox virus challenge. *J. Infect. Dis.* **181**, 10–19 (2000).
39. C. Lucas *et al.*, Yale IMPACT Team, Longitudinal analyses reveal immunological misfiring in severe COVID-19. *Nature* **584**, 463–469 (2020).
40. M. D. de Jong *et al.*, Fatal outcome of human influenza A (H5N1) is associated with high viral load and hypercytokinemia. *Nat. Med.* **12**, 1203–1207 (2006).
41. R. A. García-Ramírez *et al.*, TNF, IL6, and IL1B polymorphisms are associated with severe influenza A (H1N1) virus infection in the Mexican population. *PLoS One* **10**, e0144832 (2015).
42. J. A. Rutigliano, B. S. Graham, Prolonged production of TNF-alpha exacerbates illness during respiratory syncytial virus infection. *J. Immunol.* **173**, 3408–3417 (2004).
43. L. W. Moreland *et al.*, Long-term safety and efficacy of etanercept in patients with rheumatoid arthritis. *J. Rheumatol.* **28**, 1238–1244 (2001).
44. V. Strand *et al.*, Comparison of health-related quality of life in rheumatoid arthritis, psoriatic arthritis and psoriasis and effects of etanercept treatment. *Ann. Rheum. Dis.* **71**, 1143–1150 (2012).
45. M. Dukhinova, E. Kokinos, P. Kuchur, A. Komissarov, A. Shtro, Macrophage-derived cytokines in pneumonia: Linking cellular immunology and genetics. *Cytokine Growth Factor Rev.* **59**, 46–61 (2021).

MICROBIOLOGY

46. G. U. Meduri *et al.*, Persistent elevation of inflammatory cytokines predicts a poor outcome in ARDS. Plasma IL-1 beta and IL-6 levels are consistent and efficient predictors of outcome over time. *Chest* **107**, 1062–1073 (1995).
47. J. F. Pittet *et al.*, TGF-beta is a critical mediator of acute lung injury. *J. Clin. Invest.* **107**, 1537–1544 (2001).
48. F. Huaux *et al.*, A profibrotic function of IL-12p40 in experimental pulmonary fibrosis. *J. Immunol.* **169**, 2653–2661 (2002).
49. Z. Z. Pan, L. Parkyn, A. Ray, P. Ray, Inducible lung-specific expression of RANTES: Preferential recruitment of neutrophils. *Am. J. Physiol. Lung Cell. Mol. Physiol.* **279**, L658–L666 (2000).
50. E. M. Schmidt *et al.*, Selective blockade of tumor necrosis factor receptor I inhibits proinflammatory cytokine and chemokine production in human rheumatoid arthritis synovial membrane cell cultures. *Arthritis Rheum.* **65**, 2262–2273 (2013).
51. P. Charles *et al.*, Regulation of cytokines, cytokine inhibitors, and acute-phase proteins following anti-TNF-alpha therapy in rheumatoid arthritis. *J. Immunol.* **163**, 1521–1528 (1999).
52. R. Malaviya *et al.*, Attenuation of nitrogen mustard-induced pulmonary injury and fibrosis by anti-tumor necrosis factor-α antibody. *Toxicol. Sci.* **148**, 71–88 (2015).
53. T. Hussell, A. Pennycook, P. J. Openshaw, Inhibition of tumor necrosis factor reduces the severity of virus-specific lung immunopathology. *Eur. J. Immunol.* **31**, 2566–2573 (2001).
54. D. R. Morris *et al.*, Selective blockade of TNFR1 improves clinical disease and bronchoconstriction in experimental RSV infection. *Viruses* **12**, 1176 (2020).
55. X. Shi *et al.*, Inhibition of the inflammatory cytokine tumor necrosis factor-alpha with etanercept provides protection against lethal H1N1 influenza infection in mice. *Crit. Care* **17**, R301 (2013).
56. S. Schütze, K. Wiegmann, T. Machleidt, M. Krönke, TNF-induced activation of NF-kappa B. *Immunobiology* **193**, 193–203 (1995).
57. Z. Zhong, Z. Wen, J. E. Darnell Jr., Stat3: A STAT family member activated by tyrosine phosphorylation in response to epidermal growth factor and interleukin-6. *Science* **264**, 95–98 (1994).
58. B. C. McFarland, G. K. Gray, S. E. Nozell, S. W. Hong, E. N. Benveniste, Activation of the NF-κB pathway by the STAT3 inhibitor JSI-124 in human glioblastoma cells. *Mol. Cancer Res.* **11**, 494–505 (2013).
59. A. C. Kalil *et al.*, ACTT-2 Study Group Members, Baricitinib plus remdesivir for hospitalized adults with Covid-19. *N. Engl. J. Med.* **384**, 795–807 (2021).
60. T. Narasaraju *et al.*, Combination therapy with hepatocyte growth factor and oseltamivir confers enhanced protection against influenza viral pneumonia. *Curr. Mol. Med.* **14**, 690–702 (2014).
61. S. Pulavendran *et al.*, Combination therapy targeting platelet activation and virus replication protects mice against lethal influenza pneumonia. *Am. J. Respir. Cell Mol. Biol.* **61**, 689–701 (2019).
62. Y. N. Lai *et al.*, Combinations of 1,8-cineol and oseltamivir for the treatment of influenza virus A (H3N2) infection in mice. *J. Med. Virol.* **89**, 1158–1167 (2017).
63. D. F. Smee, A. Dagley, E. B. Tarbet, Combinations of L-N^G-monomethyl-arginine and oseltamivir against pandemic influenza A virus infections in mice. *Antivir. Chem. Chemother.* **25**, 11–17 (2017).
64. K. B. Walsh *et al.*, Suppression of cytokine storm with a sphingosine analog provides protection against pathogenic influenza virus. *Proc. Natl. Acad. Sci. U.S.A.* **108**, 12018–12023 (2011).
65. I. Solovic *et al.*, The risk of tuberculosis related to tumour necrosis factor antagonist therapies: A TBNET consensus statement. *Eur. Respir. J.* **36**, 1185–1206 (2010).
66. D. M. Nathan, P. W. Angus, P. R. Gibson, Hepatitis B and C virus infections and anti-tumor necrosis factor-alpha therapy: Guidelines for clinical approach. *J. Gastroenterol. Hepatol.* **21**, 1366–1371 (2006).
67. A. T. Russo *et al.*, An overview of tecovirimat for smallpox treatment and expanded anti-orthopoxvirus applications. *Expert Rev. Anti Infect. Ther.* **19**, 331–344 (2021).
68. A. Berhanu *et al.*, Treatment with the smallpox antiviral tecovirimat (ST-246) alone or in combination with ACAM2000 vaccination is effective as a postsymptomatic therapy for monkeypox virus infection. *Antimicrob. Agents Chemother.* **59**, 4296–4300 (2015).
69. M. Shale, M. Czub, G. G. Kaplan, R. Panaccione, S. Ghosh, Anti-tumor necrosis factor therapy and influenza: Keeping it in perspective. *Therap. Adv. Gastroenterol.* **3**, 173–177 (2010).
70. H. Körner *et al.*, Distinct roles for lymphotoxin-α and tumor necrosis factor in organogenesis and spatial organization of lymphoid tissue. *Eur. J. Immunol.* **27**, 2600–2609 (1997).
71. A. Alejo *et al.*, Chemokines cooperate with TNF to provide protective anti-viral immunity and to enhance inflammation. *Nat. Commun.* **9**, 1790 (2018).
72. G. Chaudhri, G. Kaladimou, P. Pandey, G. Karupiah, Propagation and purification of ectromelia virus. *Curr. Protoc. Microbiol.* **51**, e65 (2018).
73. C. Mavian *et al.*, The genome sequence of ectromelia virus Naval and Cornell isolates from outbreaks in North America. *Virology* **462–463**, 218–226 (2014).
74. H. Davarinejad, Quantifications of western blots with ImageJ. www.yorku.ca/yisheng/Internal/Protocols/ImageJ.pdf. Accessed 28 June 2021.